Inorganic Chemistry

Article

pubs.acs.org/IC

Mechanically Triggered Fluorescence/Phosphorescence Switching in the Excimers of Planar Trinuclear Copper(I) Pyrazolate Complexes

Qiong Xiao,[†] Ji Zheng,[†] Mian Li, Shun-Ze Zhan, Jun-Hao Wang, and Dan Li*

Department of Chemistry and Key Laboratory for Preparation and Application of Ordered Structural Materials of Guangdong Province, Shantou University, Guangdong 515063, People's Republic of China

Supporting Information

ABSTRACT: Luminescence mechanochromism of the well-known Cu_3Pz_3-type (Pz = pyrazolate) complexes is reported here, which is unusual for this family. Two types of new Cu_3Pz_3 complexes, namely $Cu_3(EBPz)_3$ (**1**; EBPz = ethyl-4′-benzoate-3,5-dimethylpyrazolate) and $Cu_3(MBPz)_3$ (polymorphs **2a**–**c**; MBPz = methyl-4′-benzoate-3,5-dimethylpyrazolate), have been synthesized and characterized. Their crystal structures exhibit a similar chairlike dimer stacking supported by short Cu···Cu contacts, which would facilitate the formation of photoinduced excimers. The dual emission from the organic fluorophore and excimeric copper cluster phosphor is found to undergo mechanically induced intensity switching between their high-energy (HE) and low-energy (LE) bands. Specifically, the relative intensities of crystalline samples are HE > LE, while the ground solid samples show LE > HE, resulting in the overall emission color interchanging between bluish violet and red. This switching can be reversed by application of solvent to the ground samples, presumably due to recrystallization, and also by heating. TD-DFT calculations reveal that the emissive singlet ligand localized state (S_1) and triplet cluster centered state (T_8) lie close in energy (separated by a gap of 0.1788 eV), suggesting the feasibility of dual emission and the possibility of reverse intersystem crossing, consistent with the long fluorescent lifetimes (10^2 ns scale) of the HE bands.

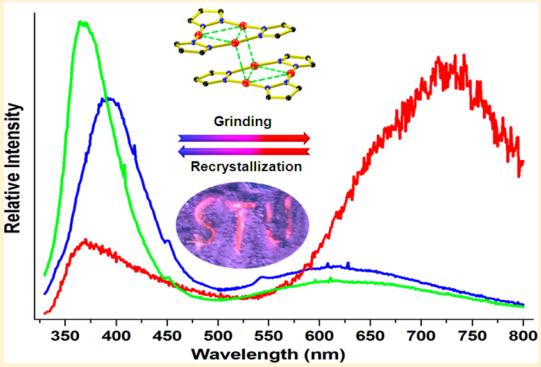

INTRODUCTION

Stimuli-responsive materials are capable of reversibly switching their readout signals in response to external factors, facilitating some applications such as sensors, memory, and displays.[1] In particular, ordered molecular materials which exhibit mechanically induced luminescence changes, including liquid crystals,[1a] dye-doped polymers,[1b] and crystalline solids (including organic compounds[1a] and coordination complexes[1c−e]), have garnered topical research interest. On the other hand, in the field of luminescent coordination complexes,[2,3] an actively pursued topic is the switching between fluorescence and phosphorescence, owing to its potential in boosting the efficiency of white organic light-emitting devices (WOLEDs).[4] An effective strategy for modulating fluorescence/phosphorescence is the dual-emitting concept implemented through device fabrication,[4b] single-component emitter design,[4c] and host−guest chemistry.[4d]

Several mechanochromic luminescent metal complexes have been synthesized and studied.[1e,5−7] The majority of them are Au^I and Pt^{II} complexes,[5,6] from which it is clear that the intra- or intermolecular metal−metal bonding can be reinforced by grinding, thus giving strong phosphorescence and mechanochromism. For Cu^I complexes, the first report of luminescence mechanochromism, which is based on a classical $Cu_4I_4P_4$-type cluster, was as late as 2010 by Perruchas et al.[7a] Shan et al. later showed the multiresponsive behaviors, including similar mechanochromism, of two new types of Cu_8I_8 and Cu_4I_4 clusters based on a phosphine ligand.[7b,c] Wen et al. have recently reported the observations of grinding-triggered luminescence changes of some copper(I) imidazolate/tetrazolate coordination polymers.[7d−f] Most recently, Perruchas and co-workers have provided an in-depth study to account for the origin of the mechanochromic properties of the $Cu_4I_4P_4$-type cluster by monitoring the grinding-induced Cu···Cu bond shortening via solid-state NMR spectra.[7g]

Our group has been interested in a family of Cu_3(pyrazolate)$_3$ complexes (abbreviated as Cu_3Pz_3).[8−20] Although the synthesis and structure of the first complex in the Cu_3Pz_3 family were documented as early as 1988 by Raptis and Fackler,[8a] continuous attention has been paid to the modification of the pyrazole skeleton, the diversity of supramolecular aggregates or adducts, and their structural and spectral characterization, owing to the contributions of many groups.[8b,c,9−11,14,16,17] Recently, it has been demonstrated, through the works of the Dias, Omary,[12] and Aida[13] groups, that Cu_3Pz_3-type complexes can exhibit rich photophysical and photochemical properties, including luminescence thermochromism, solvatochromism, and concentration luminochromism.[12b,c] Our group,[15] since 2006, has reported the first[15a] and

Received: July 15, 2014
Published: October 22, 2014

   dx.doi.org/10.1021/ic5016687 | *Inorg. Chem.* 2014, 53, 11604−11615

a series of functional metal−organic frameworks based on the Cu_3Pz_3 motif as the building blocks[15b,d−f,j] (also later by others[18]), the first[15c] Cu_3Pz_3-based coordination cage (also a larger cage by the Thiel group in the same year[19a] and later by the Yang and Raptis group[19b]) and its extension into a Cu_6Pz_6−Cu_2I_2−Cu_6Pz_6 supramolecular cluster,[15i] and also the modulation of intermolecular and nanoscale aggregation in thienyl-substituted Au_3Pz_3 complexes which exhibit dual emission.[15g,h]

Interestingly, although Cu_3Pz_3-type complexes possess a planar configuration and thus tend to form photoinduced excimers[20] showing low-energy (LE) phosphorescent emissions, which is similar to the well-known Pt^{II} complexes[6] with mechanochromic properties, there is yet no report on luminescence mechanochromism for all Cu_3Pz_3-type complexes.[8−20] This is probably because the solid-state phosphorescence of most Cu_3Pz_3-type complexes already lies in the LE region (orange or red emission). Therefore, the grinding, which is supposed to shorten the Cu···Cu bonds, is very difficult for inducing a visual luminescence change shifting to even lower energy. In this work, two types of new Cu_3Pz_3 complexes decorated with methyl or ethyl benzoate groups have been prepared. The para ester group, acting as an auxochrome, can intensify the light absorption of the organic fluorophore and hence boosts a ligand-localized high-energy (HE) band. Such a ligand modification results in unusual dual emission in this system, in which the relative intensities of the fluorescent HE and phosphorescent LE bands can be reversibly adjusted, simply through destroying/restoring the crystallinity of the bulk samples of the complexes. We also have performed DFT and TD-DFT calculations to clarify the origin of the dual emission by examining the singlet and triplet excited state ordering and absorption transitions.

EXPERIMENTAL AND COMPUTATIONAL SECTION

Materials and Measurements. The reagents and solvents employed were commercially available and were used as received. Infrared spectra were obtained as KBr disks on a Nicolet Avatar 360 FTIR spectrometer in the range of 4000−400 cm^{-1}; abbreviations used for the IR bands are w = weak, m = medium, b = broad, and vs = very strong. ^1H NMR spectroscopy was performed with a Bruker DPX 400 spectrometer using $Si(CH_3)_4$ as the internal standard. All δ values are given in ppm. Elemental analyses were carried out with Elementar Vario EL Cube equipment. Thermogravimetric measurements were performed on a TA Instruments Q50 Thermogravimetric Analyzer under a nitrogen flow of 40 mL min^{-1} at a typical heating rate of 10 °C min^{-1}. Differential scanning calorimetry (DSC) was performed on a TA-Q100 calorimeter (TA Instruments). Powder X-ray diffraction (PXRD) experiments were performed on a D8 Advance X-ray diffractometer. UV−vis absorption spectra were recorded with an Agilent 8453 UV−vis spectrophotometer (Agilent Technologies Co. Ltd.). Raman spectra were performed by 532 nm laser excitation with a LabRAM HP800 Raman spectrometer (HORIBA Jobin Yvon). Steady state photoluminescence spectra and lifetime measurements were performed with a single-photon counting spectrometer on an Edinburgh FLS920 spectrometer equipped with a continuous Xe900 xenon lamp, a μF900 μs flash lamp, and a closed cycle cryostat (Advanced Research Systems).

Synthesis of the Ligand. The ligand 4-(ethyl-4′-benzoate)-3,5-dimethyl-1*H*-pyrazole (*H*EBPz) was synthesized according to the literature,[21] but with some modification. A mixture of ethyl 4-iodobenzoate (10 mmol, 2.76 g), acetylacetone (30 mmol, 3 mL), CuI (1 mmol, 0.19 g), L-proline (2 mmol, 0.23 g), and K_2CO_3 (40 mmol, 5.53 g) in 80 mL of DMSO was heated to 90 °C under a nitrogen atmosphere for 17 h. The cooled solution was poured into HCl solution (1 M, 200 mL) and then extracted with EtOAc (10 × 100 mL). The organic phase was concentrated under reduced pressure to give a brown oily residue. Flash column chromatography (EtOAc/petroleum ether 1/20 v/v) separated out the intermediate product as a pale oil. The oily residue was added to ethanol (50 mL) and treated with an excess of hydrazine (80%, 7 mL). The solution was stirred and heated at a reflux temperature of 70 °C for 15 h, and then most of the solvent was removed using a rotary evaporator. After that, the residual colorless solution was poured into icy water (200 mL). The precipitated white solid was filtered off and dried to give 1.2 g of *H*EBPz (yield: 49%). IR (KBr pellet, cm^{-1}): 3174 (b), 3072 (w), 2978 (b), 2932 (w), 1710 (vs), 1609 (vs), 1578 (w), 1530 (s), 1460 (m), 1384 (s), 1275 (s), 1179 (m), 1104 (s), 1041 (w), 1007 (s), 865 (m), 784 (m), 710 (m), 637 (w), 542 (w), 505 (w), 483 (w). ^1H NMR (400 MHz, $CDCl_3$, 298 K): δ 8.09 (d, J = 8.2 Hz, 2H, CH_{Ph}), 7.35 (d, J = 8.1 Hz, 2H, CH_{Ph}), 4.40 (q, J = 7.1 Hz, 2H, CH_2), 2.32 (s, 6H, CH_3), 1.41 (t, J = 7.1 Hz, 3H, CH_3).

Synthesis of Complexes. *$Cu_3(C_{14}H_{15}N_2O_2)_3$ (1).* *H*EBPz (4.88 mg, 0.02 mmol) and $Cu(NO_3)_2{\cdot}3H_2O$ (4.82 mg, 0.02 mmol) were loaded into a heavy-walled glass tube, and then a solution of ethanol (2.5 mL) was added. The tube was then flame-sealed and heated to 140 °C in a programmable oven for 48 h, followed by slow cooling (5 °C/h) to room temperature. Colorless crystals were collected and air-dried. Yield: 70.1% (based on ligand). IR (KBr pellet, cm^{-1}): 2976 (w), 2913 (w), 2360 (w), 1710 (s), 1608 (s), 1543 (m), 1491 (m), 1427 (m), 1367 (w), 1273 (s), 1177 (m), 1105 (s), 1016 (m), 855 (w), 770 (m), 706 (w), 568 (w), 519 (w). Anal. Calcd for $C_{42}H_{45}Cu_3N_6O_6$: C, 54.80; H, 4.93; N, 9.13. Found: C, 54.78; H, 4.73; N, 9.22. ^1H NMR (400 MHz, $CDCl_3$, 298 K): δ 8.09 (d, J = 8.4 Hz, 2H, CH_{Ph}), 7.35 (d, J = 8.4 Hz, 2H, CH_{Ph}), 4.40 (q, J = 7.1 Hz, 2H, CH_2), 2.38 (s, 6H, CH_3), 1.42 (t, J = 7.1 Hz, 3H, CH_3); after grinding: δ 8.08 (d, J = 8.4 Hz, 2H, CH_{Ph}), 7.35 (d, J = 8.4 Hz, 2H, CH_{Ph}), 4.40 (q, J = 7.1 Hz, 2H, CH_2), 2.38 (s, 6H, CH_3), 1.42 (t, J = 7.1 Hz, 3H, CH_3).

*$Cu_3(C_{13}H_{13}N_2O_2)_3$ (**2a**).* *H*EBPz (4.48 mg, 0.02 mmol) and Cu_2O (4.3 mg, 0.03 mmol) were loaded into a heavy-walled glass tube, and then a solution of methanol (2.5 mL) was added. The tube was then flame-sealed and heated to 140 °C in a programmable oven for 48 h, followed by slow cooling (5 °C/h) to room temperature. Colorless crystals were collected and air-dried. Yield: 54.7% (based on ligand). IR (KBr pellet, cm^{-1}): 2946 (w), 2909 (w), 1716 (s), 1608 (s), 1543 (m), 1491 (m), 1431 (m), 1345 (w), 1273 (s), 1179 (m), 1106 (s), 859 (w), 771 (m), 706 (w), 564 (w), 512 (w). Anal. Calcd for $C_{39}H_{39}Cu_3N_6O_6$: C, 53.33; H, 4.48; N, 9.57. Found: C, 53.35; H, 4.34; N, 9.66. ^1H NMR (400 MHz, $CDCl_3$, 298 K): δ 8.08 (d, J = 8.4 Hz, 2H, CH_{Ph}), 7.35 (d, J = 7.4 Hz, 2H, CH_{Ph}), 3.94 (s, 3H, CH_3), 2.37 (s, 6H, CH_3); after grinding: δ 8.08 (d, J = 8.4 Hz, 2H, CH_{Ph}), 7.35 (d, J = 8.4 Hz, 2H, CH_{Ph}), 3.94 (s, 3H, CH_3), 2.38 (s, 6H, CH_3).

*$Cu_3(C_{13}H_{13}N_2O_2)_3$ (**2b**).* *H*EBPz (4.48 mg, 0.02 mmol) and Cu_2O (4.3 mg, 0.03 mmol) were loaded into a heavy-walled glass tube, and then a mixed solution of methanol (1 mL), toluene (0.25 mL), and acetonitrile (1 mL) was added. The tube was then flame-sealed and heated to 140 °C in a programmable oven for 48 h, followed by slow cooling (5 °C/h) to room temperature. Colorless crystals were collected and air-dried. Yield: 38.6% (based on ligand). IR (KBr pellet, cm^{-1}): 2949 (w), 2914 (w), 1717 (s), 1608 (s), 1543 (m), 1492 (m), 1432 (m), 1344 (w), 1274 (s), 1180 (m), 1108 (s), 1015 (m), 859 (w), 771 (m), 708 (w), 568 (w), 516 (w). Anal. Calcd for $C_{39}H_{39}Cu_3N_6O_6$: C, 53.33; H, 4.48; N, 9.57. Found: C, 53.32; H, 4.35; N, 9.53. ^1H NMR (400 MHz, $CDCl_3$, 298 K): δ 8.09 (d, J = 8.1 Hz, 2H, CH_{Ph}), 7.35 (d, J = 8.3 Hz, 2H, CH_{Ph}), 3.94 (s, 3H, CH_3), 2.40 (s, 6H, CH_3); after grinding, δ 8.08 (d, J = 8.2 Hz, 2H, CH_{Ph}), 7.34 (d, J = 8.2 Hz, 2H, CH_{Ph}), 3.94 (s, 3H, CH_3), 2.37 (s, 6H, CH_3).

*$Cu_3(C_{13}H_{13}N_2O_2)_3$ (**2c**).* *H*EBPz (4.48 mg, 0.02 mmol), Cu_2O (4.3 mg, 0.03 mmol), and $Cu(NO_3)_2{\cdot}3H_2O$ (3.9 mg, 0.016 mmol) were loaded into a heavy-walled glass tube, and then a mixed solution of methanol (1 mL), toluene (0.25 mL), and acetonitrile (1 mL) was added. The tube was then flame-sealed and heated to 140 °C in a programmable oven for 48 h, followed by slow cooling (5 °C/h) to room temperature. Colorless crystals were collected and air-dried. Yield: 43.2% (based on ligand). IR (KBr pellet, cm^{-1}): 2950 (w), 2913 (w), 2360 (w), 1719 (s), 1608 (s), 1543 (m), 1492 (m), 1433 (m),

dx.doi.org/10.1021/ic5016687 | *Inorg. Chem.* 2014, 53, 11604−11615

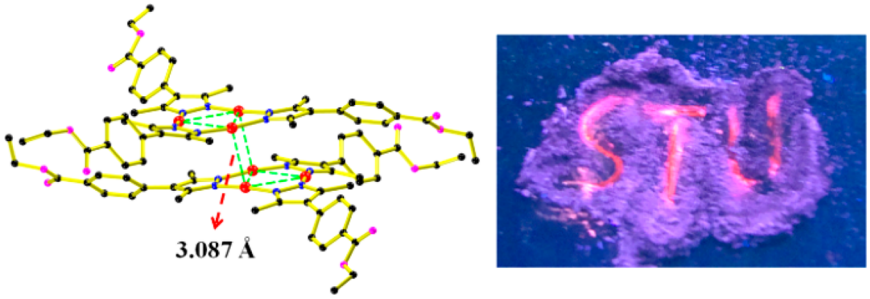

Figure 1. (left) Dimer stacking pattern in the crystal structure of **1** (color code: Cu in red, N in blue, C in black, O in pink, H omitted, Cu···Cu bonds in green). (right) The letters "STU" written with a spatula on the sample of **1** cast on filter paper under 254 nm UV light under ambient conditions.

1341 (w), 1275 (s), 1180 (m), 1109 (s), 1015 (m), 859 (w), 773 (w), 706 (w), 568 (w). Anal. Calcd for $C_{39}H_{39}Cu_3N_6O_6$: C, 53.33; H, 4.48; N, 9.57. Found: C, 53.51; H, 4.50; N, 9.65. ^{1}H NMR (400 MHz, $CDCl_3$, 298 K): δ 8.07 (d, J = 8.3 Hz, 2H, CH_{Ph}), 7.33 (d, J = 8.2 Hz, 2H, CH_{Ph}), 3.94 (s, 3H, CH_3), 2.32 (s, 6H, CH_3); after grinding: δ 8.07 (d, J = 8.2 Hz, 2H, CH_{Ph}), 7.34 (d, J = 8.2 Hz, 2H, CH_{Ph}), 3.94 (s, 3H, CH_3), 2.36 (s, 6H, CH_3).

Caution! In the synthesis of complexes **1** and **2**, the volume of the solution should not exceed one-third of the volume of the glass tubes to avoid overloading. Be careful and avoid potential empyrosis and incised wound when flame-sealing and opening the glass tubes.

Crystal Structure Determination. Suitable crystals of complexes **1** and **2** were mounted with glue at the end of a glass fiber. Data collection was performed with an Oxford Diffraction Gemini E instrument (Enhance Cu X-ray source, Kα, λ = 1.54056 Å) equipped with a graphite monochromator and ATLAS CCD detector (CrysAlis CCD, Oxford Diffraction Ltd.) at room temperature (293 K). Structures were solved by direct methods (SHELXTL-97) and refined on F^2 using full-matrix least squares (SHELXTL-97).[22] All non-hydrogen atoms were refined with anisotropic thermal parameters, and all hydrogen atoms were included in calculated positions and refined with isotropic thermal parameters riding on those of the parent atoms. Crystal data and structure refinement parameters are summarized in Table S1 (Supporting Information). Selected bond lengths and angles are given in Tables S2–S5 in the Supporting Information. CCDC nos. 964376–964379.

Computational Details. DFT and TD-DFT calculations were performed by using the PBE0 method.[23] The Lanl2dz[24] effective core potential (ECP) was applied for Cu, while the 6-31G(d,p)[25] basis set was used for C, N, O, and H atoms. The Gaussian 09 A.02[26] software package was used for all calculations. All models for the calculations were taken from the atomic coordinates from the X-ray diffraction data without optimization. Both the monomer (the two crystallographically independent $Cu_3(EBPz)_3$ molecules in **1** and the only $Cu_3(MBPz)_3$ molecule in **2c**) and dimer (that formed from the $Cu_3(EBPz)_3$ molecules with Cu1, Cu2, and Cu3 in **1**) models were considered. The first 60 singlet–singlet spin-allowed transitions were calculated by TD-DFT for all four models and were further treated by SWizard 4.6[27] software to obtain the simulated UV–vis absorption spectra (Gaussian distribution, half-bandwidth 500 cm^{-1}). The first 30 singlet–triplet spin-forbidden transitions for one of the monomer models (that with Cu1, Cu2, and Cu3 in **1**) and the first 50 singlet–triplet spin-forbidden transitions for the dimer model (that formed from Cu1, Cu2, and Cu3 in **1**) were also calculated by TD-DFT. Because in the calculations the spin–orbital coupling was not considered, the singlet–triplet transitions all have zero oscillator strength. The molecular orbital compositions were obtained by the Hirshfeld method[28] and by using Multiwfn 3.3.3[29] software. Most of the detailed computational results are given in the Supporting Information.

RESULTS AND DISCUSSION

Synthesis, Crystallization, and Grinding. The ethyl 4′-benzoate substituted ligand *H*EBPz was presynthesized for the preparation of $Cu_3(EBPz)_3$ (**1**), while methyl 4′-benzoate-3,5-dimethyl-pyrazolate (MBPz) was formed in situ via an ester exchange reaction (from EBPz to MBPz in the presence of methanol) during the generation of $Cu_3(MBPz)_3$ (**2**). The formation of the methyl ester group was confirmed by the ^{1}H NMR spectrum of **2**, in which the chemical shift of the methylene group is absent and that of the methyl group shifts downfield (from δ 1.42 to 3.94 ppm), in comparison with that of **1**.

The crystalline samples of **1** and **2** were prepared by the solvothermal method. Interestingly, when the copper sources (Cu_2O or $Cu(NO_3)_2{\cdot}3H_2O$) and the solvents (methanol or mixed methanol/toluene/acetonitrile) were varied, three polymorphs of $Cu_3(MBPz)_3$ (namely, **2a–c**) were generated. It should be mentioned that, under solvothermal conditions, the in situ reduction of Cu^{II} to Cu^{I} has been well documented.[30] A polymorph of **1** has been recently reported.[18d] The purity of all four samples has been demonstrated by elemental analysis, IR and ^{1}H NMR spectra, and PXRD patterns (Figure S1 in the Supporting Information). The possibility of solvent molecules inclusion is ruled out by elemental analysis and thermogravimetric analysis, which shows no weight loss before the thermal decomposition temperature up to above 300 °C (Figure S2 in the Supporting Information).

The single crystals of all four samples were obtained, and then their structures were determined by X-ray crystallographic analysis (Table S1 in the Supporting Information). For **1** and **2**, a similar dimer stacking pattern supported by chairlike Cu···Cu contacts is observed in the cyclic trinuclear structures (that of **1** is shown in Figure 1, left; others are given in Figure S3 in the Supporting Information). The intermolecular Cu···Cu distances (**1**, 3.087, 3.175 Å; **2a**, 3.135, 3.141 Å; **2b**, 3.123, 3.168 Å; **2c**, 3.088 Å; see Table S6 in the Supporting Information for intramolecular Cu···Cu distances and ∠N–Cu–N bond angles) in the dimers are much shorter than that (3.58 Å) of the Cu_3Pz_3 complex with the 4-phenyl-3,5-dimethylpyrazolate ligand[17b] and slightly longer than that (2.95 Å, Cu···Cu van der Waals radii sum 2.8 Å) of $Cu_3(3,5\text{-}Me_2Pz)_3$ (3,5-Me_2Pz = 3,5-dimethylpyrazolate).[12c,15a] The ∠N–Cu–N bond angles, ranging from 172 to 177°, are slightly distorted relative to the ideal linear coordination geometry of two-coordinated copper(I) ion, probably because of the attraction of intertrimeric Cu···Cu contacts.

We noted that the bulk sample of **1** showed bluish violet emission under a UV lamp; this is different from the case for previously reported Cu_3Pz_3-type complexes, which usually showed orange or red emission in the solid state.[12,15] Remarkably, by simple grinding of a sample of **1** with a spatula

dx.doi.org/10.1021/ic5016687 | Inorg. Chem. 2014, 53, 11604–11615

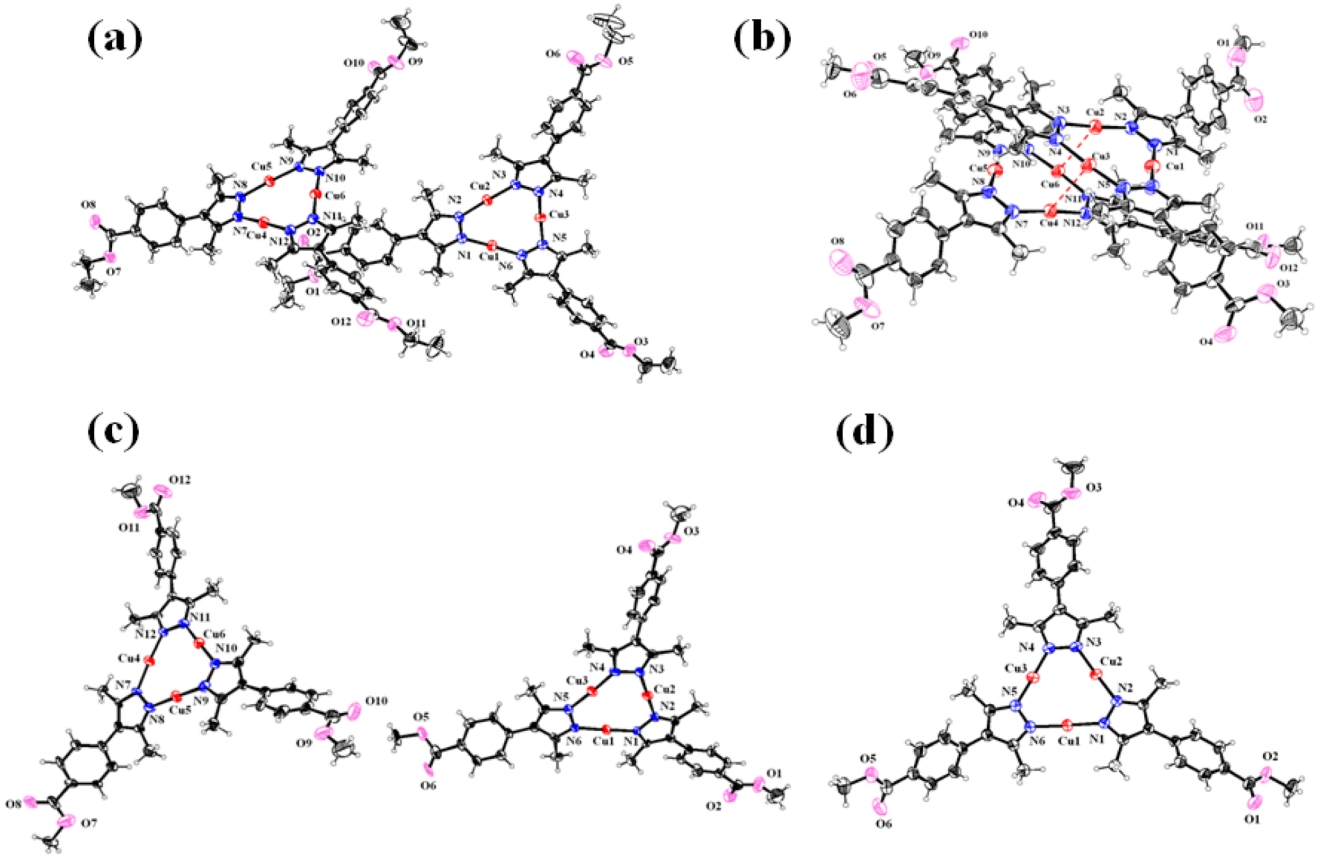

Figure 2. Crystallographically asymmetric units (with 30% thermal ellipsoids) of **1** (a) and polymorphs **2a** (b), **2b** (c), and **2c** (d). Color code: Cu in red, N in blue, C in black, O in pink, H in gray.

Table 1. Summary of Crystal-Packing Modes in 1 and Polymorphs 2a–c

complex	monomer	dimer	layer
1	A, B	A–A, B–B	A–A···B–B···A–A
2a	A, B	A–B	A–B···B–A···A–B
2b	A, B	A–A, B–B	A–A···A–A···A–A, B–B···B–B···B–B
2c	A	A–A	A–A···A–A···A–A

Codes: A: monomer with Cu1, Cu2 and Cu3; B: monomer with Cu4, Cu5 and Cu6; "–": intermolecular Cu···Cu bonding; "···": intermolecular Cu···O weak interaction.

under UV light, a high-contrast visual emission change from bluish violet to red occurred immediately (Figure 1, right). Such a phenomenon is not observed for $Cu_3(3,5\text{-}Me_2Pz)_3$,[12c,15a] despite its even shorter Cu···Cu bonds. It was also reported for the 4-phenyl Cu_3Pz_3 complex[17b] that, even when an external pressure of up to 3.18 GPa was applied, the strengthened Cu···Cu interaction only caused the enhancement of the emission intensity, without luminescence mechanochromism.

Crystal Structures and Polymorphism. Although the dimer stacking pattern exists in **1** and **2**, all of which exhibit notably short intermolecular Cu···Cu bonds, there are subtle differences on the crystal packing for the four crystal structures. They crystallize in four different space groups (Table S1 in the Supporting Information). For the asymmetric units (Figure 2), there are two symmetry-independent trinuclear molecules (monomer) for **1** and **2a**,**b** but only one for **2c**. Herein we label the trinuclear molecule with Cu1, Cu2, and Cu3 in each complex as monomer A and that with Cu4, Cu5, and Cu6 as monomer B (Table 1). Interestingly, the chairlike dimers are formed through a centrosymmetric operation in **1**, and **2b**,**c**; in comparison, the dimer in **2a** consists of two symmetry-independent monomers. In other words, the dimer stacking mode is A–A and B–B in **1** and **2b**, A–A in **2c**, and A–B in **2a** (Table 1). As a result, there is only one type of Cu···Cu distance for **2c** and two types for the other three complexes.

Another structural feature responsible for the different crystal packings in **1** and **2** is the intermolecular Cu···O interaction between dimers. The interacting distances (ranging from 3.19 to 3.55 Å; see Table S7 in the Supporting Information) and directions of these weak forces between carbonyl O and Cu^I ions are similar for **1** and **2**. Therefore, only those of **1** are shown here (Figure 3; see Figures S4–S7 in the Supporting Information for a comparison of **1** and **2**). In **1**, the carbonyl O sites from adjacent dimers are located on both sides above the exposed Cu_3 planes for both dimers A–A and B–B (Figure 3a,b). Such an interacting mode can be described as a π acid–base interaction.[12e] Each dimer is connected to four adjacent dimers to construct a two-dimensional (2-D) supramolecular

dx.doi.org/10.1021/ic5016687 | *Inorg. Chem.* 2014, 53, 11604–11615

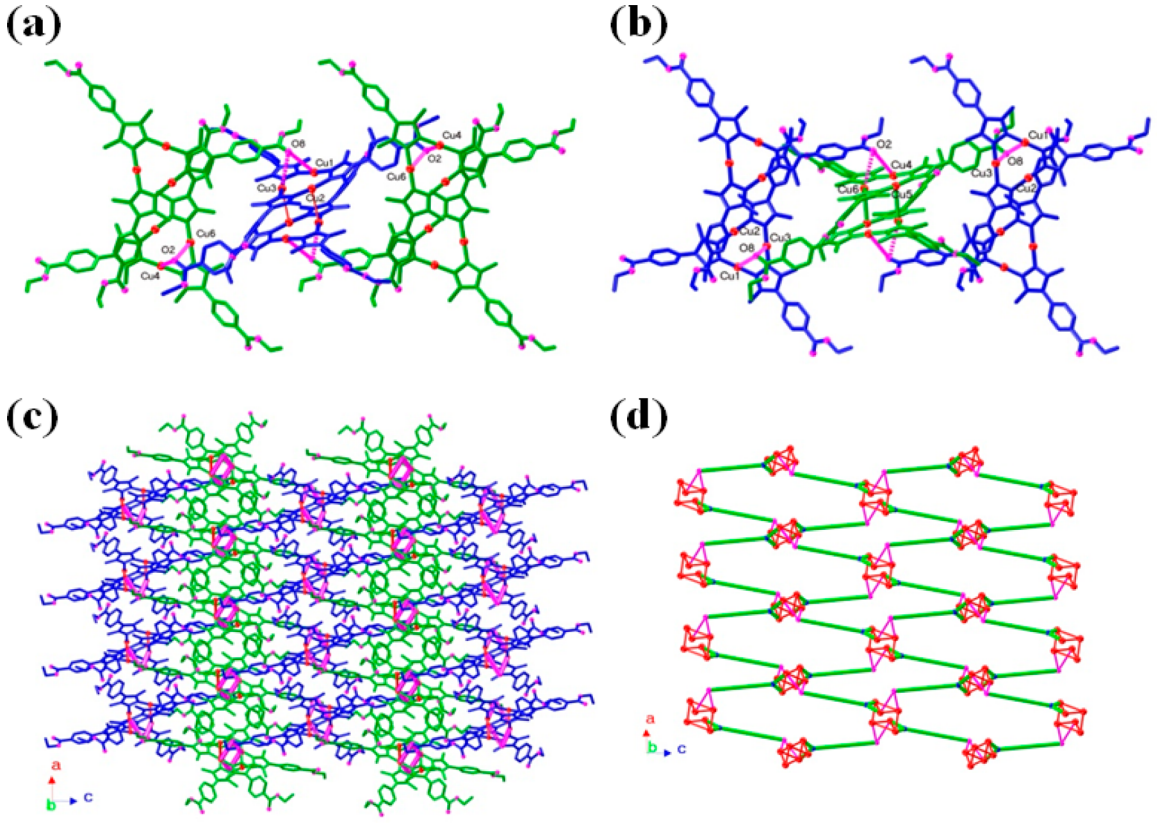

Figure 3. Structural diagrams of **1**, showing the intermolecular Cu···O weak interactions around dimer A–A (a) and dimer B–B (b) and a top view of one 2-D supramolecular layer (c) and its simplified network (d). Color code: monomer A in blue, monomer B in green, Cu and Cu···Cu bonds in red, O and Cu···O interactions in pink; in (d) the ligands are simplified to green lines.

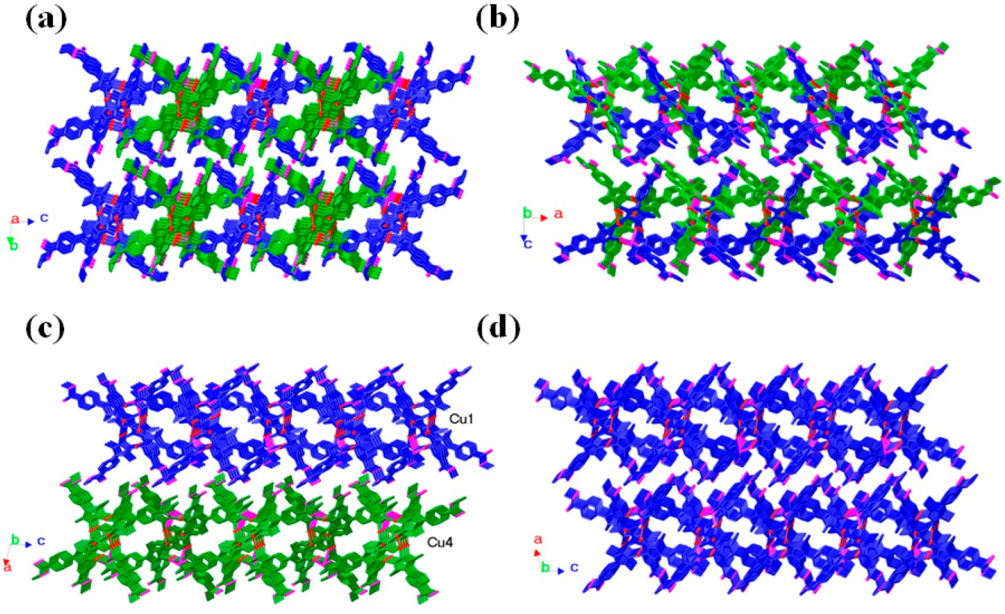

Figure 4. Crystal packing diagrams of **1** (a) and polymorphs **2a** (b), **2b** (c) and **2c** (d), showing the side views of the 2-D supramolecular layers in which monomers A are highlighted in blue and monomers B in green (Cu in red, O in pink).

layer (Figure 3c), and thus a simple (4,4)-grid type network can be envisaged (Figure 3d).

Although the interaction modes and distances of the Cu···O weak interactions are similar, the combinations of dimers through these interactions are diverse for all four cases (Figure 4), as summarized in Table 1. For example, in **1** and **2b**, dimers A–A and B–B both exist. However, for **1** the two types of dimers are further arranged in an alternating fashion (B···A–A···B and A···B–B···A) through Cu···O interactions in one supramolecular layer (Figure 4a); in contrast, for **2b** the same type of dimers propagate in one layer, thus generating two

dx.doi.org/10.1021/ic5016687 | *Inorg. Chem.* 2014, 53, 11604–11615

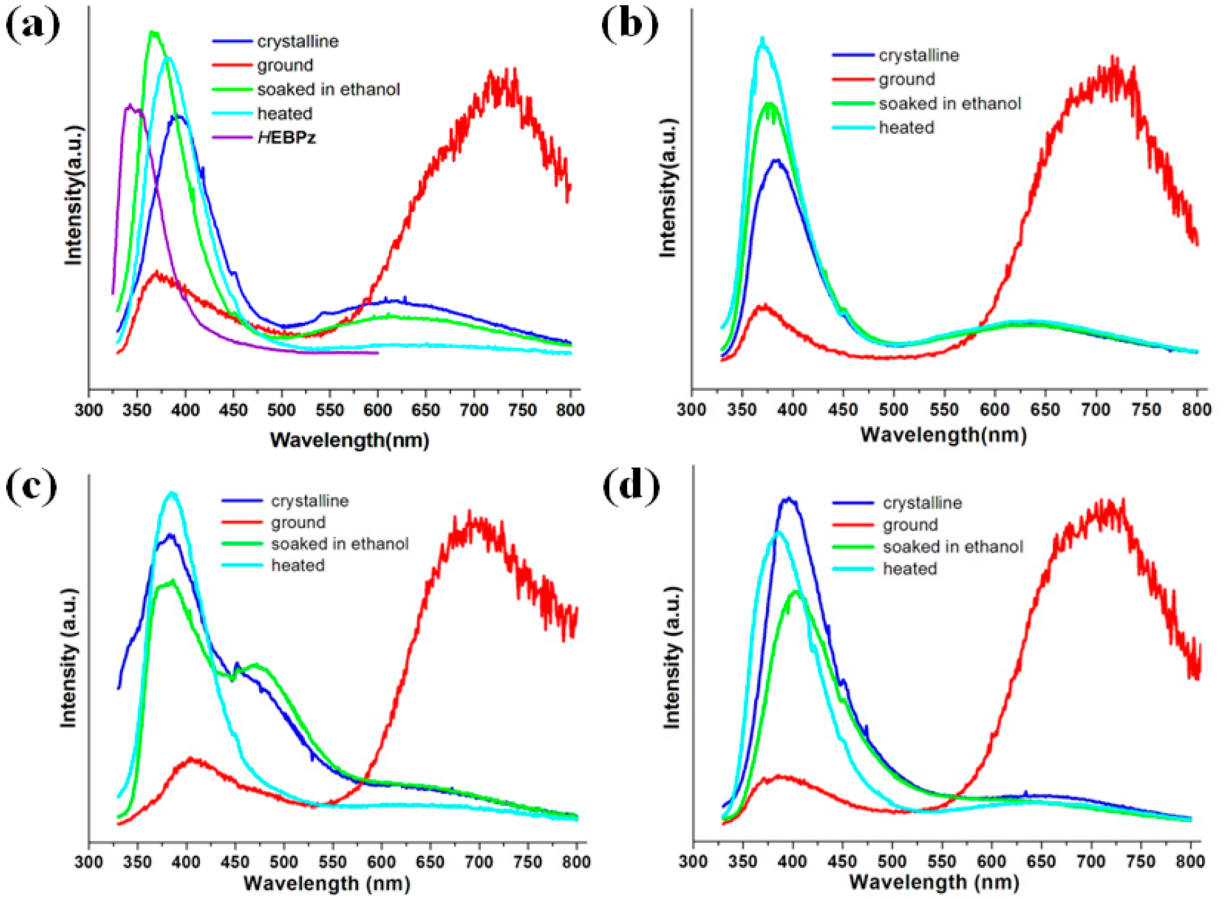

Figure 5. Solid-state emission spectra of **1** (a), **2a** (b), **2b** (c), **2c** (d), and *H*EBPz (a) before and after grinding the samples of the complexes and subsequent soaking in ethanol or heating.

symmetry-independent 2-D layers which are alternately packed in the overall crystal structure (Figure 4c).

It is also noted that the phenyl and pyrazolyl rings deviate significantly from coplanarity, indicating that the conjugation effect between these two moieties is reduced, and thus the ligand-based luminescence, with the aid of the para esteryl auxochrome, is expected to be of higher energy (i.e., blue shifted). For example, the phenyl−pyrazolyl dihedral angles in **1** are ranging from 35 to 56°. No significant difference in these values is found for **1** and **2** (Tables S2−S5 in the Supporting Information). For the 4-phenyl Cu_3Pz_3 complex, the phenyl−pyrazolyl angle is also as large as ca. 46°,[17b] suggesting that such a deviation may not arise from the intermolecular Cu···O interactions.

Solid-State Dual Emission. On dissolution in $CHCl_3$ solvent, all complexes showed similar bluish violet emissions (peaks at ca. 390 nm) in the HE region, almost identical with that of the ligand *H*EBPz (Figure S8 in the Supporting Information). The lack of phosphorescent LE bands is probably due to the quenching effect of triplet oxygen in solution, which is common in this family of complexes.[15g,h] In the solid state, similar intense HE bands were observed for all complexes, but with slight red shifts relative to that of *H*EBPz (Figure 5; see also Figure S9 in the Supporting Information for corresponding excitation spectra), because the crystal-packing effect may enhance the rigidity of the benzoate−pyrazolate motif and stabilize the $\pi\pi^*$ states. In contrast, the LE bands are much weaker, which is unusual for the excimer of $(Cu_3Pz_3)_2$ with such short Cu···Cu contacts.[12,15,20] The emission peaks of the HE and LE bands and their relative intensities and decay lifetimes are summarized in Table 2.

Table 2. Solid-State Dual Emission Peaks, Relative Intensities, and Lifetimes of 1 and 2

complex	λ_{em}^{max} (nm)[a]	HE/LE[b]	τ_1 (μs)[c]	τ_2 (μs)[d]
1	390, 620/370, 730	4.0/0.28	0.75/0.73	10.71/20.21
2a	390, 630/370, 710	4.8/0.19	0.83/0.78	13.47/29.46
2b	380, 630/400, 700	7.4/0.21	0.75/0.78	15.69/27.60
2c	390, 650/380, 710	10.6/0.16	0.78/0.81	24.60/28.60

[a]HE and LE emission peaks. [b]Relative intensities of HE/LE bands (see Table S8 in the Supporting Information). [c]Decay lifetimes of HE bands monitored at emission peaks. [d]Decay lifetimes of LE bands monitored at emission peaks (see Table S9 in the Supporting Information). The slants separate the measurements before and after grinding the crystalline samples.

From the temperature-dependent (50−293 K) emission spectra (Figure S10 in the Supporting Information), there is no obvious thermochromism[12b−d,15e,f,i] related to the major HE and LE bands, but a notable shoulder at ca. 500 nm appears at low temperatures in all cases. We tentatively assume that there are multiple ligand-based emissive states in the solid state due to crystal packing effects, which are subject to thermal equilibration and are only manifested under cryogenic conditions. We observe that this shoulder is most obvious for **2b**, in comparison with those of **2a**,**c**. Interestingly, for these three polymorphs, **2b** exhibits the most complicated crystal

dx.doi.org/10.1021/ic5016687 | Inorg. Chem. 2014, 53, 11604−11615

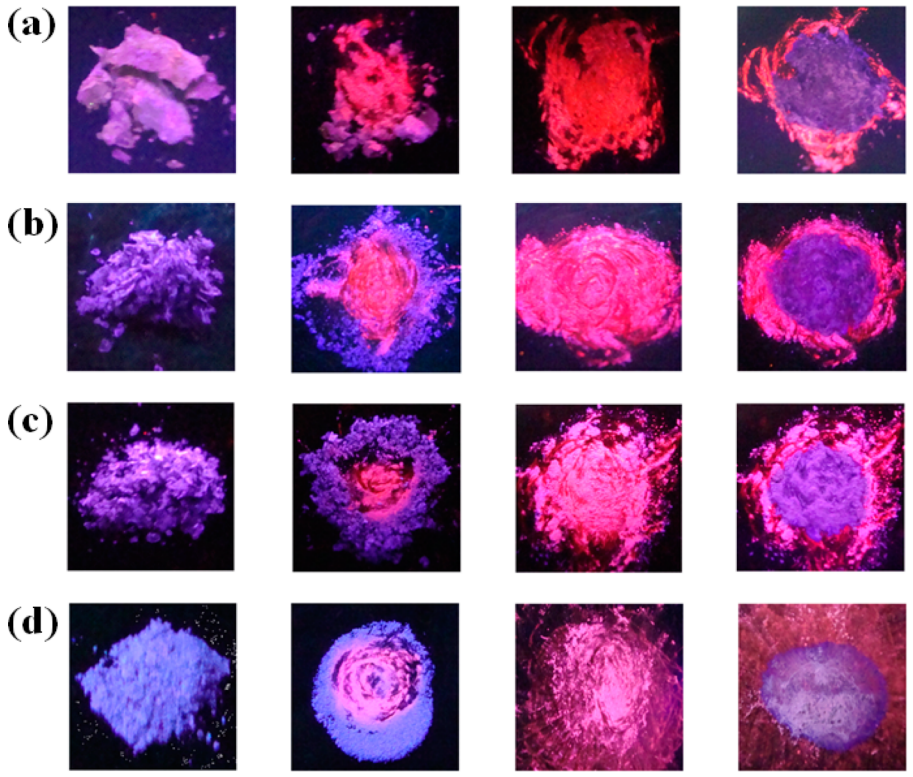

Figure 6. Photographs of samples of **1** (a), **2a** (b), **2b** (c) and **2c** (d) under a 254 nm UV lamp. From left to right: crystalline sample; partially ground sample; thoroughly ground sample; sample treated with ethanol after grinding.

structure, showing an alternating layer packing mode (Figure 4c and Table 1), as discussed above.

The decay lifetimes of the LE bands lie in the microsecond scale (ca. 10−25 μs; see Table 2), indicating phosphorescence, typical for Cu_3Pz_3-type complexes. Importantly, the coexistence of the HE emission is highly unusual, because in an electronically excited molecule only the lowest excited state of a given multiplicity can emit photons in appreciable yield (known as Kasha's rule[31]). Therefore, the HE bands, which are ligand-based, should originate from the singlet excited states. However, in light of the fact that the decay lifetimes of the HE bands lie in the range of ca. 0.7−0.8 μs for **1** and **2** (see Table 2), significantly longer than the fluorescence lifetimes (in the order of 1 ns) of common organic compounds, there may be two possible origins for this ligand-localized emission.[32] The first possible consideration is an origin of ligand-based $^{1,3}\pi\pi^*$ states, for which the intersystem crossing times can be as long as 0.1−1 μs.[32a] The second consideration, recently proposed by Yersin and co-workers for some Cu^I complexes,[32a] is the possibility of reverse intersystem crossing and thermally activated delayed fluorescence.[33,34] For this second mechanism, a prerequisite is that the energy separation between the emissive singlet and triplet states should be rather small (on the order of 10^2 cm^{-1}) and close to the thermal activation energy k_BT at ambient temperature.[32a,33,34] This point will be evaluated in Origins of Dual Emission.

Luminescence Mechanochromism and Fluorescence/Phosphorescence Switching. The crystalline samples of **1** and **2** can all show luminescence mechanochromism, with their emission color switching between bluish violet and red (Figure 6). Taking **1** as an example (Figure 6a), when the crystals were ground in a mortar under UV light, the violet emission changed to intense red, and then, simply after the addition of several drops of ethanol to the ground sample, the color can reversibly switch back to violet. This process can be repeated for several cycles.

The grinding-induced emission color switching corresponds to the drastic variation of the relative intensities of the HE and LE bands in the emission spectra of **1** and **2** (Figure 5 and Table 2). Specifically, the relative intensities of crystalline samples are HE > LE, while the ground solid samples show LE > HE. After grinding, the LE bands become dominant for all cases, and the LE lifetimes also become longer, while those of HE emission stay largely the same (see Table 2). Such a phenomenon is attributed to the possible shortening of the intermolecular Cu···Cu bonds through mechanical stimuli. Although more evidence is needed in the present system, there are consistent speculations from previous reports that mechanical stimuli can cause the contraction of metal···metal bonds and hence reinforce the phosphorescence from the triplet metal−metal (^{3}MM) states.[5−7] In particular, convincing structural evidence has been recently given in which a drastic contraction of Au···Au contacts (from 5.733 to 3.177 Å) is determined in a single-crystal to single-crystal manner and simply triggered by pricking the crystal of phenyl(phenyl isocyanide)gold(I).[5j] Most recently, through the subtle comparison of a pair of polymorphic $Cu_4I_4P_4$-type complexes, the grinding-induced Cu···Cu bonding contraction has also been successfully monitored by ^{31}P and ^{6S}Cu solid-state NMR spectra.[7g]

The recovery of HE bands in the emission spectra can be achieved by soaking the ground samples in ethanol and also by heating them to 130 °C for 2 h (Figure 5). The intensities of the recovered HE bands are even stronger than those of the original crystalline samples. We note that for **2b** (Figure 5c) the shoulder at ca. 500 nm, which is also observed in the

dx.doi.org/10.1021/ic5016687 | *Inorg. Chem.* 2014, 53, 11604−11615

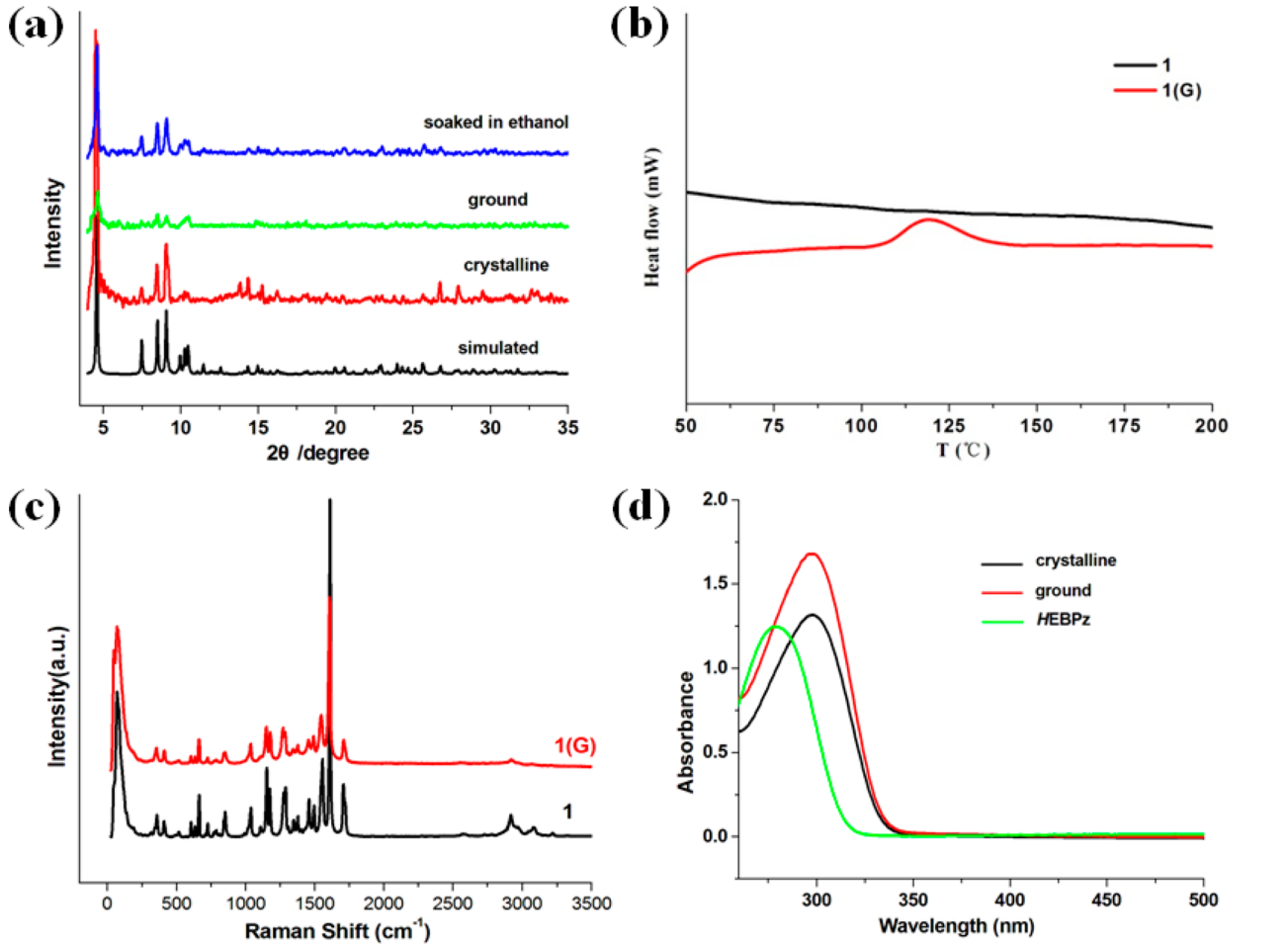

Figure 7. Simulated and experimental (before and after grinding, and then soaking in ethanol) PXRD patterns (a), DSC measurements (b), Raman spectra (c), and UV−vis absorption spectra in solution (d) of **1** before and after grinding (denoted "G").

aforementioned temperature-dependent emission spectra (Figure S10c in the Supporting Information), has been fully recovered when the ground sample is treated with ethanol, while for the heating method, this shoulder is absent. The reason for such an observation could be very complicated, but it is possible that the soaking method induces recrystallization and hence reproduces the crystal-packing effect, while the heating method may fail to do so.

Reversible Crystal to Amorphous Phase Transition. The reversible process of destroying/restoring the crystallinity of the samples has been demonstrated by powder X-ray diffraction (PXRD) measurements (Figure 7a and Figure S1 in the Supporting Information). The crystal to amorphous transition is confirmed by the severely reduced intensity of the diffraction peaks, and the subsequent recrystallization by using the soaking method is evident in the recovery of these peaks. The almost unaltered ^{1}H NMR spectra (Figure S11 in the Supporting Information) of the samples before and after grinding show that the trinuclear cluster structures are preserved for all complexes.

For the heating recovery method, it is shown, by differential scanning calorimetry (DSC) measurements, that there exists an exothermic peak covering 110−140 °C for the ground samples, which is absent for the crystalline samples (Figure 7b and Figure S12 in the Supporting Information), indicating that a new kind of phase transition may occur at high temperature. The Raman spectral measurements are supposed to monitor the variation of the strength of Cu···Cu bonding before and after grinding.[35] Unfortunately, there is no detectable distinction for those of **1** and **2** on application to 532 nm laser excitation in our equipment (Figure 7c and Figure S13 in the Supporting Information), probably because the excitation energy is too low. We also show that no new absorption band occurs after grinding, according to the UV−vis absorption spectra in $CHCl_3$ solution (Figure 7d and Figure S14 in the Supporting Information).

Origins of Dual Emission. Previous theoretical studies[12d,15c,17b,20] have consistently shown that, for those undecorated Cu_3Pz_3-type complexes, the major electronic transitions responsible for the LE band are exactly or mostly from the HOMO (d(Cu) and/or pπ(Pz) orbital) to the LUMO (spσ(Cu···Cu) orbital), indicating the population of the cluster-centered triplet ^{3}MM emissive states. In contrast, the occurrence of the additional, strong HE emission bands in **1** and **2** suggests that a set of new, strong absorption transitions, which are related to the ligand-localized excited states, might appear.

Preliminary DFT and TD-DFT calculations have been performed to look into the origins of the dual emission. We have first considered the monomer models (which are computationally more economical) to evaluate the influence of the subtle conformational difference caused by crystal packing effects, which is crucial for the absorption strength of the ligand-based HE states, as we found recently.[15g] Therefore,

dx.doi.org/10.1021/ic5016687 | Inorg. Chem. 2014, 53, 11604−11615

both the A and B monomers (Figure 2a) in **1** are included. To consider the influence of different ligands (EBPz or MBPz), the monomer A (Figure 2d) in **2c** (the simplest polymorph) is also included. The results indicate that the molecular orbital contours (Figure S15 in the Supporting Information), orbital energy levels (Figure S16 in the Supporting Information), absorption transitions (Table S10 and S11 in the Supporting Information), and simulated absorption spectra (Figure S17 in the Supporting Information) are qualitatively analogous for the three monomers. It should be mentioned that the monomer model is only appropriate for discussing the ligand-localized HE emission; the dimer model must be used when the cluster-centered LE emission is under consideration, especially when the intermolecular Cu···Cu distances are very short, such as in the cases of **1** and **2**.

We then focus on the dimer model (A–A) in **1** to gain a photophysical interpretation for this dual-emitting system. The molecular orbital contours and energy levels (Figure 8; see also Figure S18 in the Supporting Information for more orbitals) and their quantitative Hirshfeld compositions (Table 3; see also Table S12 in the Supporting Information for all data) are calculated. It is found that the typical orbitals responsible for the cluster-centered LE band are now pushed to the HOMO-4/-5 and LUMO+6 orbitals, while those between these two orbitals are mainly ligand-based π or π^* orbitals. The simulated singlet–singlet electronic transitions (Table 3; see also Table S13 in the Supporting Information for all data) and absorption spectrum (Figure S19 in the Supporting Information) reveal that the ligand-centered S_1 state, which has a very strong absorption strength, involves the HOMO → LUMO ($p\pi$-(EBPz)/d(Cu) → $p\pi$(EBPz)*) transition. In contrast, the major cluster-centered transition, HOMO-5 → LUMO+6 (d(Cu)/$p\pi$(EBPz) → $sp\sigma$(Cu···Cu)/σ^*(Pz)), is found in a higher-lying singlet excited state (S_{36}), with a much smaller oscillator strength. This could explain the much weaker LE band, relative to the HE band, before grinding.

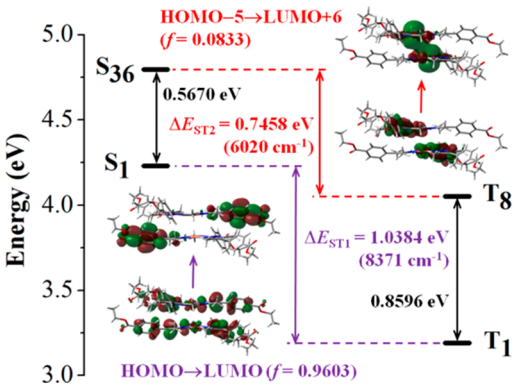

Figure 8. Energy levels and ordering of the singlet and triplet excited states related to the HE (S_1 and T_1) and LE (S_{36} and T_8) bands for the A–A dimer in **1**. The inserted orbitals are from the major transitions responsible for the HE (marked in purple) and LE (marked in red) bands, respectively (f = oscillator strength).

The singlet–triplet transitions (Table 3; see also Table S14 in the Supporting Information for more data) are also calculated for evaluating the singlet–triplet energy separation (ΔE_{ST}),[32] which is closely related to the aforementioned reverse intersystem crossing and thermally activated delayed fluorescence.[33,34] The HOMO → LUMO transition is also found in the lowest triplet state (T_1), while HOMO-5 → LUMO+6 is involved in a higher-lying triplet state (T_8). Three important findings can be outlined from Figure 8. (i) The ΔE_{ST} value for the cluster-centered state is smaller than that of the ligand-centered state (i.e., $\Delta E_{ST2} < \Delta E_{ST1}$, both on the order of several 10^3 cm^{-1}). The ΔE_{ST} value is small if the involved orbitals in the transitions have a small spatial overlap.[32c] This can be traced to the newly generated intermolecular $sp\sigma$(Cu···Cu) bonding in LUMO+6. (ii) Although the energy gap between the triplet T_1 to T_8 (0.8596 eV) is larger than that between the singlet S_1 to S_{36} (0.5670 eV), there are many more in-between states from the singlet S_1 to S_{36}. Because the effective population of T_8 would require the spin–orbital coupling with the higher-lying singlet states (those with specific electronic configuration similar to that of T_8),[32c] the large number of in-between singlet states may facilitate the intersystem crossing process. (iii) Remarkably, it is noted that the two major emissive states, S_1 and T_8, are close in energy (separated by only 0.1788 eV; i.e. 1438 cm^{-1}). Although such an energy separation is slightly larger than the requirement (on the order of 10^2 cm^{-1}) of the thermally activated delayed fluorescence speculated above,[32a,33,34] the possibility of partial reverse intersystem crossing could not be ruled out, which provides a basis for the fluorescence/phosphorescence switching.

Table 3. Selected Excited States of the A–A Dimer in 1 and Their Electronic Properties

excited state	energy (nm)[a]	f[b]	absorption transition[c]	orbital composition (%)[d]
S_1	293.1	0.9603	H → L (60%), H-1 → L+1 (18%), H-1 → L+3 (8%)	HOMO: Cu, 16.96; Pz, 53.73; Me, 2.71; Ph, 24.10; Es, 2.50
T_1	388.4	N/A	H → L (21%), H-1 → L+1 (18%), H-1 → L+3 (9%), H-3 → L (8%), H-9 → L (6%)	LUMO: Cu, 2.47; Pz, 10.52; Me, 1.91; Ph, 59.35; Es, 25.75
S_{36}	258.4	0.0833	H-5 → L+6 (29%), H-1 → L+5 (19%), H-5 → L (6%)	HOMO-5: Cu, 43.55; Pz, 38.63; Me, 3.01; Ph, 13.54; Es, 1.28
T_8	306	N/A	H-5 → L+6 (24%), H → L+6 (14%), H-9 → L+6 (12%), H-10 → L+12 (8%)	LUMO+6: Cu, 65.71; Pz, 22.18; Me, 8.40; Ph, 3.28; Es, 0.43

[a]Energy levels calculated from the vertical transition energies from TD-DFT and without excited-state geometric optimization (see Tables S13 and S14 in the Supporting Information for other excited states). [b]Oscillator strengths of vertical transitions (N/A: not available for triplet excited states because spin–orbital coupling is not considered). [c]Corresponding absorption transitions and their contributions to the population of excited states (the population percentages are calculated by $2 \times |c|^2 \times 100\%$, where c is the transition coefficient). Abbreviations: H, HOMO; L, LUMO. [d]Hirshfeld compositions of the fragments of the molecular orbitals related to the largest-contribution absorption transitions (see Table S12 in the Supporting Information for other orbitals). Abbreviations: Pz, pyrazolyl; Me, methyl; Ph, phenyl; Es, esteryl.

dx.doi.org/10.1021/ic5016687 | Inorg. Chem. 2014, 53, 11604–11615

CONCLUSION

In conclusion, the observation and characterization of luminescence mechanochromism for the well-known $(Cu_3Pz_3)_2$ clusters are reported in this work. These complexes are different from previously reported Cu_3Pz_3-type complexes because switchable dual emission is unusual for molecular luminescent systems. The addition of the para esteryl auxochrome appears to be a useful way for inducing dual emission in this system. Crystal-packing effects, albeit effective in producing several polymorphs and subtly influencing the emission bands, do not significantly vary the luminescence mechanochromism properties in this work.

The experimental and theoretical results suggest that the ligand-centered S_1 and cluster-centered T_8 excited states are the major origins of the HE and LE bands, respectively, and also reveal that these two excited states lie close in energy, which is the prerequisite for the observed fluorescence/phosphorescence switching.

It should be mentioned that the intrinsic difficulty in fully understanding the luminescence mechanochromism in this system remains the monitoring and modeling of the subtle geometric changes during the mechanically triggered crystal to amorphous transition, especially the intermolecular Cu···Cu distance variation which is crucial for the enhancement of the phosphorescence. Further spectral measurements, such as ultrafast time-resolved transient absorption and resonance Raman spectroscopy, could be insightful. On the other hand, more in-depth calculations, which take into account the spin−orbital coupling and excited-state geometric optimization, are ongoing.

ASSOCIATED CONTENT

Supporting Information

Figures, tables, and CIF files giving X-ray crystallographic data for complexes **1** and **2a−c**, crystal structures, additional measurements and figures, and computational results. This material is available free of charge via the Internet at http://pubs.acs.org.

AUTHOR INFORMATION

Corresponding Author

*E-mail for D.L.: dli@stu.edu.cn.

Author Contributions

†These authors contributed equally.

Notes

The authors declare no competing financial interest.

ACKNOWLEDGMENTS

This work was financially supported by the National Basic Research Program of China (973 Program, Nos. 2013CB834803 and 2012CB821706) and the National Natural Science Foundation of China (Nos. 21171114 and 91222202).

REFERENCES

(1) For reviews, see: (a) Sagara, Y.; Kato, T. *Nat. Chem.* **2009**, *1*, 605. (b) Theato, P.; Sumerlin, B. S.; O'Reilly, R. K.; Epps, T. H., III *Chem. Soc. Rev.* **2013**, *42*, 7055. (c) Balch, A. *Angew. Chem., Int. Ed.* **2009**, *48*, 2641. (d) Wenger, O. S. *Chem. Rev.* **2013**, *113*, 3686. (e) Zhang, X.; Chi, Z.; Zhang, Y.; Liu, S.; Xu, J. *J. Mater. Chem. C* **2013**, *1*, 3376.

(2) For reviews of luminescent Cu(I) complexes, see: (a) Ford, P. C.; Cariati, E.; Bourassa, J. *Chem. Rev.* **1999**, *99*, 3625. (b) Armaroli, N.; Accorsi, G.; Cardinali, F.; Listorti, A. *Top. Curr. Chem.* **2007**, *280*, 69. (c) Wallesch, M.; Volz, D.; Zink, D. M.; Schepers, U.; Nieger, M.; Baumann, T.; Bräse, S. *Chem. Eur. J.* **2014**, *20*, 6578.

(3) For reviews of other luminescent metal complexes, see: (a) Yersin, H. *Top. Curr. Chem.* **2004**, *241*, 1. (b) Lai, S.-W.; Che, C.-M. *Top. Curr. Chem.* **2004**, *241*, 27. (c) Balzani, V.; Bergamini, G.; Campagna, S.; Puntoriero, F. *Top. Curr. Chem.* **2007**, *280*, 1. (d) Yam, V. W.-W.; Cheng, E. C.-C. *Chem. Soc. Rev.* **2008**, *37*, 1806. (e) Chi, Y.; Chou, P.-T. *Chem. Soc. Rev.* **2010**, *39*, 638.

(4) (a) Sun, Y.; Giebink, N. C.; Kanno, H.; Ma, B.; Thompson, M. E.; Forrest, S. R. *Nature* **2006**, *440*, 908. (b) Yan, B.-P.; Cheung, C. C. C.; Kui, S. C. F.; Xiang, H.-F.; Roy, V. A. L.; Xu, S.-J.; Che, C.-M. *Adv. Mater.* **2007**, *19*, 3599. (c) Zhang, G.; Palmer, G. M.; Dewhirst, M. W.; Fraser, C. L. *Nat. Mater.* **2009**, *8*, 747. (d) Sun, C.-Y.; Wang, X.-L.; Zhang, X.; Qin, C.; Li, P.; Su, Z.-M.; Zhu, D.-X.; Shan, G.-G.; Shao, K.-Z.; Wu, H.; Li, J. *Nat. Commun.* **2013**, *4*, 2717. (e) Choy, W. C. H.; Chan, W. K.; Yuan, Y. *Adv. Mater.* **2014**, *26*, 5368.

(5) Au(I) complexes: (a) Assefa, Z.; Omary, M. A.; McBurnett, B. G.; Mohamed, A. A.; Patterson, H. H.; Staples, R. J.; Fackler, J. P. *Inorg. Chem.* **2002**, *41*, 6274. (b) Lee, Y.-A.; Eisenberg, R. *J. Am. Chem. Soc.* **2003**, *125*, 7778. (c) Schneider, J.; Lee, Y.-A.; Pérez, J.; Brennessel, W. W.; Flaschenriem, C.; Eisenberg, R. *Inorg. Chem.* **2008**, *47*, 957. (d) Ito, H.; Saito, T.; Oshima, N.; Kitamura, N.; Ishizaka, S.; Hinatsu, Y.; Wakeshima, M.; Kato, M.; Tsuge, K.; Sawamura, M. *J. Am. Chem. Soc.* **2008**, *130*, 10044. (e) Kuchison, A. M.; Wolf, M. O.; Patrick, B. O. *Chem. Commun.* **2009**, 7387. (f) Osawa, M.; Kawata, I.; Igawa, S.; Hoshino, M.; Fukunaga, T.; Hashizume, D. *Chem. Eur. J.* **2010**, *16*, 12114. (g) Laguna, A.; Lasanta, T.; López-de-Luzuriaga, J. M.; Monge, M.; Naumov, P.; Olmos, M. E. *J. Am. Chem. Soc.* **2010**, *132*, 456. (h) Lasanta, T.; Olmos, M. E.; Laguna, A.; López-de-Luzuriaga, J. M.; Naumov, P. *J. Am. Chem. Soc.* **2011**, *133*, 16358. (i) Koshevoy, I. O.; Lin, C.-L.; Karttunen, A. J.; Haukka, M.; Shih, C.-W.; Chou, P.-T.; Tunik, S. P.; Pakkanen, T. A. *Chem. Commun.* **2011**, *47*, 5533. (j) Ito, H.; Muromoto, M.; Kurenuma, S.; Ishizaka, S.; Kitamura, N.; Sato, H.; Seki, T. *Nat. Commun.* **2013**, *4*, 2009. (k) Seki, T.; Sakurada, K.; Ito, H. *Angew. Chem., Int. Ed.* **2013**, *52*, 12828. (l) Jobbágy, C.; Deák, A. *Eur. J. Inorg. Chem.* **2014**, 4434 and references therein.

(6) Pt(II) complexes: (a) Kozhevnikov, V. N.; Donnio, B.; Bruce, D. W. *Angew. Chem., Int. Ed.* **2008**, *47*, 6286. (b) Abe, T.; Itakura, T.; Ikeda, N.; Shinozaki, K. *Dalton Trans.* **2009**, 711. (c) Nishiuchi, Y.; Takayama, A.; Suzuki, T.; Shinozaki, K. *Eur. J. Inorg. Chem.* **2011**, 1815. (d) Ni, J.; Zhang, X.; Wu, Y.-H.; Zhang, L.-Y.; Chen, Z.-N. *Chem. Eur. J.* **2011**, *17*, 1171. (e) Ni, J.; Zhang, X.; Qiu, N.; Wu, Y.-H.; Zhang, L.-Y.; Zhang, J.; Chen, Z.-N. *Inorg. Chem.* **2011**, *50*, 9090. (f) Zhang, X.; Wang, J.-Y.; Ni, J.; Zhang, L.-Y.; Chen, Z.-N. *Inorg. Chem.* **2012**, *51*, 5569. (g) Choi, S. J.; Kuwabara, J.; Nishimura, Y.; Arai, T.; Kanbara, T. *Chem. Lett.* **2012**, *41*, 65. (h) Huang, L.-M.; Tu, G.-M.; Chi, Y.; Hung, W.-Y.; Song, Y.-C.; Tseng, M.-R.; Chou, P.-T.; Lee, G.-H.; Wong, K.-T.; Cheng, S.-H.; Tsai, W.-S. *J. Mater. Chem. C* **2013**, *1*, 7582. (i) Ohba, T.; Kobayashi, A.; Chang, H.-C.; Kato, M. *Dalton Trans.* **2013**, *42*, 5514. (j) Ni, J.; Wang, Y.-G.; Wang, H.-H.; Xu, L.; Zhao, Y.-Q.; Pan, Y.-Z.; Zhang, J.-J. *Dalton Trans.* **2014**, *43*, 352.

(7) Cu(I) complexes: (a) Perruchas, S.; Le Goff, X. F.; Maron, S.; Maurin, I.; Guillen, F.; Garcia, A.; Gacoin, T.; Boilot, J.-P. *J. Am. Chem. Soc.* **2010**, *132*, 10967. (b) Shan, X.-C.; Zhang, H.-B.; Chen, L.; Wu, M.-Y.; Jiang, F.-L.; Hong, M.-C. *Cryst. Growth Des.* **2013**, *13*, 1377. (c) Shan, X.-C.; Jiang, F.-L.; Chen, L.; Wu, M.-Y.; Pan, J.; Wan, X.-Y.; Hong, M.-C. *J. Mater. Chem. C* **2013**, *1*, 4339. (d) Wen, T.; Zhang, D.-X.; Liu, J.; Lin, R.; Zhang, J. *Chem. Commun.* **2013**, *49*, 5660. (e) Wen, T.; Zhang, D.-X.; Zhang, H.-X.; Zhang, H.-B.; Zhang, J.; Li, D.-S. *Chem. Commun.* **2014**, *50*, 8754. (f) Wen, T.; Zhou, X.-P.; Zhang, D.-X.; Li, D. *Chem.—Eur. J.* **2014**, *20*, 644. (g) Benito, Q.; Le Goff, X. F.; Maron, S.; Fargues, A.; Garcia, A.; Martineau, C.; Taulelle, F.; Kahlal, S.; Gacoin, T.; Boilot, J.-P.; Perruchas, S. *J. Am. Chem. Soc.* **2014**, *136*, 11311.

(8) (a) Raptis, R. G.; Fackler, J. P. *Inorg. Chem.* **1988**, *27*, 4179. (b) Ehlert, M. K.; Rettig, S. J.; Storr, A.; Thompson, R. C.; Trotter, J. *Can. J. Chem.* **1990**, *68*, 1444. (c) Ehlert, M. K.; Rettig, S. J.; Storr, A.; Thompson, R. C.; Trotter, J. *Can. J. Chem.* **1992**, *70*, 2161.

(9) (a) Ardizzoia, G. A.; La Monica, G.; Liu, C.-W; Fackler, J. P. *Inorg. Synth.* **1997**, *31*, 299. (b) Ardizzoia, G. A.; Cenini, S.; La Monica, G.; Masciocchi, N.; Maspero, A.; Moret, M. *Inorg. Chem.* **1998**, *37*, 4284. (c) Bertolotti, F.; Maspero, A.; Cervellino, A.; Guagliardi, A.; Masciocchi, N. *Cryst. Growth Des.* **2014**, *14*, 2913 and references therein for other metal pyrazolates and their applications.

(10) (a) Singh, K.; Long, J. R.; Stavropoulos, P. *J. Am. Chem. Soc.* **1997**, *119*, 2942. (b) Singh, K.; Long, J. R.; Stavropoulos, P. *Inorg. Chem.* **1998**, *37*, 1073.

(11) (a) Meyer, F.; Jacobi, A.; Zsolnai, L. *Chem. Ber.* **1997**, *130*, 1441. (b) Stollenz, M.; John, M.; Gehring, H.; Dechert, S.; Grosse, C.; Meyer, F. *Inorg. Chem.* **2009**, *48*, 10049. (c) Veronelli, M.; Kindermann, N.; Dechert, S.; Meyer, S.; Meyer, F. *Inorg. Chem.* **2014**, *53*, 2333.

(12) (a) Dias, H. V. R.; Polach, S. A.; Wang, Z. *J. Fluorine Chem.* **2000**, *103*, 163. (b) Dias, H. V. R.; Diyabalanage, H. V. K.; Rawashdeh-Omary, M. A.; Franzman, M. A.; Omary, M. A. *J. Am. Chem. Soc.* **2003**, *125*, 12072. (c) Dias, H. V. R.; Diyabalanage, H. V. K.; Eldabaja, M. G.; Elbjeirami, O.; Rawashdeh-Omary, M. A.; Omary, M. A. *J. Am. Chem. Soc.* **2005**, *127*, 7489. (d) Omary, M. A.; Rawashdeh-Omary, M. A.; Gonser, M. W. A.; Elbjeirami, O.; Grimes, T.; Cundari, T. R. *Inorg. Chem.* **2005**, *44*, 8200. (e) Tekarli, S. M.; Cundari, T. R.; Omary, M. A. *J. Am. Chem. Soc.* **2008**, *130*, 1669. (f) Hettiarachchi, C. V.; Rawashdeh-Omary, M. A.; Korir, D.; Kohistani, J.; Yousufuddin, M.; Dias, H. V. R. *Inorg. Chem.* **2013**, *52*, 13576.

(13) (a) Enomoto, M.; Kishimura, A.; Aida, T. *J. Am. Chem. Soc.* **2001**, *123*, 5608. (b) Kishimura, A.; Yamashita, T.; Yamaguchi, K.; Aida, T. *Nat. Mater.* **2005**, *4*, 546.

(14) (a) Fujisawa, K.; Ishikawa, Y.; Miyashita, Y.; Okamoto, K.-i. *Chem. Lett.* **2004**, *33*, 66. (b) Fujisawa, K.; Ishikawa, Y.; Miyashita, Y.; Okamoto, K.-i. *Inorg. Chim. Acta* **2010**, *363*, 2977.

(15) (a) He, J.; Yin, Y.-G.; Wu, T.; Li, D.; Huang, X.-C. *Chem. Commun.* **2006**, 2845. (b) Zhang, J.-X.; He, J.; Yin, Y.-G.; Hu, M.-H.; Li, D.; Huang, X.-C. *Inorg. Chem.* **2008**, *47*, 3471. (c) Gao, G.-F.; Li, M.; Zhan, S.-Z.; Lv, Z.; Chen, G.-h.; Li, D. *Chem. Eur. J.* **2011**, *17*, 4113. (d) Zhan, S.-Z.; Li, M.; Zhou, X.-P.; Li, D.; Ng, S. W. *RSC Adv.* **2011**, *1*, 1457. (e) Zhan, S.-Z.; Li, M.; Zhou, X.-P.; Wang, J.-H.; Yang, J.-R.; Li, D. *Chem. Commun.* **2011**, *47*, 12441. (f) Zhan, S.-Z.; Li, M.; Ng, S. W.; Li, D. *Chem. Eur. J.* **2013**, *19*, 10217. (g) Ni, W.-X.; Li, M.; Zheng, J.; Zhan, S.-Z.; Qiu, Y.-M.; Ng, S. W.; Li, D. *Angew. Chem., Int. Ed.* **2013**, *52*, 13472. (h) Ni, W.-X.; Qiu, Y.-M.; Li, M.; Zheng, J.; Sun, R. W.-Y.; Zhan, S.-Z.; Ng, S. W.; Li, D. *J. Am. Chem. Soc.* **2014**, *136*, 9532. (i) Wang, J.-H.; Li, M.; Zheng, J.; Huang, X.-C.; Li, D. *Chem. Commun.* **2014**, *50*, 9115. (j) Wang, J.-H.; Li, M.; Li, D. *Chem. Eur. J.* **2014**, *20*, 12004.

(16) (a) Tsupreva, V. N.; Filippov, O. A.; Titov, A. A.; Krylova, A. I.; Sivaev, I. B.; Bregadze, V. I.; Epstein, L. M.; Shubina, E. S. *J. Organomet. Chem.* **2009**, *694*, 1704. (b) Tsupreva, V. N.; Titov, A. A.; Filippov, O. A.; Bilyachenko, A. N.; Smol'yakov, A. F.; Dolgushin, F. M.; Agapkin, D. V.; Godovikov, I. A.; Epstein, L. M.; Shubina, E. S. *Inorg. Chem.* **2011**, *50*, 3325. (c) Titov, A. A.; Filippov, O. A.; Bilyachenko, A. N.; Smol'yakov, A. F.; Dolgushin, F. M.; Belsky, V. K.; Godovikov, I. A.; Epstein, L. M.; Shubina, E. S. *Eur. J. Inorg. Chem.* **2012**, 5554. (d) Titov, A. A.; Guseva, E. A.; Smol'yakov, A. F.; Dolgushin, F. M.; Filippov, O. A.; Golub, I. E.; Krylova, A. I.; Babakhina, G. M.; Epstein, L. M.; Shubina, E. S. *Russ. Chem. Bull.* **2013**, *62*, 1829. (e) Titov, A. A.; Filippov, O. A.; Guseva, E. A.; Smol'yakov, A. F.; Dolgushin, F. M.; Epstein, L. M.; Belsky, V. K.; Shubina, E. S. *RSC Adv.* **2014**, *4*, 8350.

(17) (a) Morawitz, T.; Lerner, H.-W.; Bolte, M. *Acta Crystallogr., Sect. E* **2006**, *62*, 1474. (b) Gong, F.; Wang, Q.; Chen, J.; Yang, Z.; Liu, M.; Li, S.; Yang, G.; Bai, L.; Liu, J.; Dong, Y. *Inorg. Chem.* **2010**, *49*, 1658. (c) Xu, Z.-L.; Li, H.-X.; Ren, Z.-G.; Du, W.-Y.; Xu, W.-C.; Lang, J.-P. *Tetrahedron* **2011**, *67*, 5282.

(18) (a) Zhang, J.-P.; Kitagawa, S. *J. Am. Chem. Soc.* **2008**, *130*, 907. (b) Hou, L.; Shi, W.-J.; Wang, Y.-Y.; Wang, H.-H.; Cui, L.; Chen, P.-X.; Shi, Q.-Z. *Inorg. Chem.* **2011**, *50*, 261. (c) Grzywa, M.; Geßner, C.; Denysenko, D.; Bredenkötter, B.; Gschwind, F.; Fromm, K. M.; Nitek, W.; Klemm, E.; Volkmer, D. *Dalton Trans.* **2013**, *42*, 6909. (d) Wei, Z.-W.; Yuan, D.-Q.; Zhao, X.-L.; Sun, D.-F.; Zhou, H.-C. *Sci. China Chem.* **2013**, *56*, 418.

(19) (a) Jozak, T.; Sun, Y.; Schmitt, Y.; Lebedkin, S.; Kappes, M.; Gerhards, M.; Thiel, W. R. *Chem. Eur. J.* **2011**, *17*, 3384. (b) Duan, P.-C.; Wang, Z.-Y.; Chen, J.-H.; Yang, G.; Raptis, R. G. *Dalton Trans.* **2013**, *42*, 14951.

(20) (a) Vorontsov, I. I.; Kovalevsky, A. Yu.; Chen, Y.-S.; Graber, T.; Gembicky, M.; Novozhilova, I. V.; Omary, M. A.; Coppens, P. *Phys. Rev. Lett.* **2005**, *94*, 193003. (b) Grimes, T.; Omary, M. A.; Dias, H. V. R.; Cundari, T. R. *J. Phys. Chem. A* **2006**, *110*, 5823. (c) Hu, B.; Gahungu, G.; Zhang, J. *J. Phys. Chem. A* **2007**, *111*, 4965.

(21) Jiang, Y.; Wu, N.; Wu, H.; He, M. *Synlett* **2005**, *18*, 2731.

(22) Sheldrick, G. M. *Acta Crystallogr., Sect. A* **2008**, *64*, 112.

(23) (a) Perdew, J. P.; Burke, K.; Ernzerhof, M. *Phys. Rev. Lett.* **1996**, *77*, 3865. (b) Perdew, J. P.; Burke, K.; Ernzerhof, M. *Phys. Rev. Lett.* **1997**, *78*, 1396.

(24) (a) Dunning, T. H., Jr.; Hay, P. J. In *Modern Theoretical Chemistry*; Schaefer, H. F., III., Ed.; Plenum: New York, 1976, Vol. 3, pp 1−28. (b) Hay, P. J.; Wadt, W. R. *J. .Chem. Phys.* **1985**, *82*, 270. (c) Hadt, W. R.; Hay, P. J. *J. Chem. Phys.* **1985**, *82*, 284. (d) Hay, P. J.; Wadt, W. R. *J. Chem. Phys.* **1985**, *82*, 299.

(25) Hariharan, P. C.; Pople, J. A. *Mol. Phys.* **1974**, *27*, 209.

(26) Frisch, M. J.; Trucks, G. W.; Schlegel, H. B.; Scuseria, G. E.; Robb, M. A.; Cheeseman, J. R.; Scalmani, G.; Barone, V.; Mennucci, B.; Petersson, G. A.; Nakatsuji, H.; Caricato, M.; Li, X.; Hratchian, H. P.; Izmaylov, A. F.; Bloino, J.; Zheng, G.; Sonnenberg, J. L.; Hada, M.; Ehara, M.; Toyota, K.; Fukuda, R.; Hasegawa, J.; Ishida, M.; Nakajima, T.; Honda, Y.; Kitao, O.; Nakai, H.; Vreven, T.; Montgomery, J. A., Jr.; Peralta, J. E.; Ogliaro, F.; Bearpark, M.; Heyd, J. J.; Brothers, E.; Kudin, K. N.; Staroverov, V. N.; Kobayashi, R.; Normand, J.; Raghavachari, K.; Rendell, A.; Burant, J. C.; Iyengar, S. S.; Tomasi, J.; Cossi, M.; Rega, N.; Millam, J. M.; Klene, M.; Knox, J. E.; Cross, J. B.; Bakken, V.; Adamo, C.; Jaramillo, J.; Gomperts, R.; Stratmann, R. E.; Yazyev, O.; Austin, A. J.; Cammi, R.; Pomelli, C.; Ochterski, J.;. Martin, R. L; Morokuma, K.; Zakrzewski, V. G.; Voth, G. A.; Salvador, P.; Dannenberg, J. J.; Dapprich, S.; Daniels, A. D.; Farkas, O.; Foresman, J. B.; Ortiz, J. V.; Cioslowski, J.; Fox, D. J. *GAUSSIAN 09 (Revision A.2)*; Gaussian, Inc., Wallingford, CT, 2009.

(27) (a) Gorelsky, S. I. *SWizard Program*; University of Ottawa, Ottawa, Canada, 2010. (b) Gorelsky, S. I.; Lever, A. B. P. *J. Organomet. Chem.* **2001**, *635*, 187.

(28) Hirshfeld, F. L. *Theor. Chim. Acta* **1977**, *44*, 129.

(29) (a) Lu, T. *Multiwfn, Revison 3.3.3*; University of Science and Technology Beijing, Beijing, People's Republic of China, 2014. (a) Lu, T.; Chen, F. W. *J. Comput. Chem.* **2012**, *33*, 580.

(30) Chen, X.-M.; Tong, M.-L. *Acc. Chem. Res.* **2007**, *40*, 162.

(31) (a) Kasha, M. *Faraday Soc. Discuss.* **1950**, *9*, 14. (b) Glazer, E. C.; Magde, D.; Tor, Y. *J. Am. Chem. Soc.* **2005**, *127*, 4190. (c) Glazer, E. C.; Magde, D.; Tor, Y. *J. Am. Chem. Soc.* **2007**, *129*, 8544. (d) Nishikawa, M.; Nomoto, K.; Kume, S.; Inoue, K.; Sakai, M.; Fujii, M.; Nishihara, H. *J. Am. Chem. Soc.* **2010**, *132*, 9579.

(32) (a) Yersin, H.; Rausch, A. F.; Czerwieniec, R.; Hofbeck, T.; Fischer, T. *Coord. Chem. Rev.* **2011**, *255*, 2622. (b) De Angelis, F.; Fantacci, S.; Sgamellotti, A.; Cariati, E.; Ugo, R.; Ford, P. C. *Inorg. Chem.* **2006**, *45*, 10576. (c) Lam, W. H.; Lam, E. S.-H.; Yam, V. W.-W. *J. Am. Chem. Soc.* **2013**, *135*, 15135.

(33) (a) Uoyama, H.; Goushi, K.; Shizu, K.; Nomura, H.; Adachi, C. *Nature* **2012**, *492*, 234. (b) Yao, L.; Zhang, S.; Wang, R.; Li, W.; Shen, F.; Yang, B.; Ma, Y. *Angew. Chem., Int. Ed.* **2014**, *53*, 2119. (c) Pan, Y.; Li, W.; Zhang, S.; Yao, L.; Gu, C.; Xu, H.; Yang, B.; Ma, Y. *Adv. Optical Mater.* **2014**, *2*, 510.

(34) (a) Deaton, J. C.; Switalski, S. C.; Kondakov, D. Y.; Young, R. H.; Pawlik, T. D.; Giesen, D. J.; Harkins, S. B.; Miller, A. J. M.; Mickenberg, S. F.; Peters, J. C. *J. Am. Chem. Soc.* **2010**, *132*, 9499. (b) Czerwieniec, R.; Yu, J.; Yersin, H. *Inorg. Chem.* **2011**, *50*, 8293. (c) Czerwieniec, R.; Kowalski, K.; Yersin, H. *Dalton Trans.* **2013**, *42*, 9826. (d) Zink, D. M.; Bächle, M.; Baumann, T.; Nieger, M.; Kühn, M.; Wang, C.; Klopper, W.; Monkowius, U.; Hofbeck, T.; Yersin, H.;

Bräse, S. *Inorg. Chem.* **2013**, *52*, 2292. (e) Zheng, J.; Yu, Y.-D.; Liu, F.-F.; Liu, B.-Y.; Wei, G.; Huang, X.-C. *Chem. Commun.* **2014**, *50*, 9000.
(35) (a) Che, C.-M.; Mao, Z.; Miskowski, V. M.; Tse, M.-C.; Chan, C.-K.; Cheung, K.-K.; Phillips, D. L.; Leung, K.-H. *Angew. Chem., Int. Ed.* **2000**, *39*, 4084. (b) Che, C.-M.; Lai, S.-W. *Coord. Chem. Rev.* **2005**, *249*, 1296. (c) Phillips, D. L.; Che, C.-M.; Leung, K. H.; Mao, Z.; Tse, M.-C. *Coord. Chem. Rev.* **2005**, *249*, 1476.